Solid-State Electronics 199 (2023) 108499

Contents lists available at ScienceDirect

Solid State Electronics

journal homepage: www.elsevier.com/locate/sse

Efficient and accurate defect level modeling in monolayer MoS_2 via GW+DFT with open boundary conditions☆

Guido Gandus [a,*], Youseung Lee [a], Leonard Deuschle [a], Daniele Passerone [b], Mathieu Luisier [a]

[a] Integrated Systems Laboratory, ETH Zürich, Switzerland
[b] nanotech@surfaces, EMPA, Switzerland

ARTICLE INFO

Keywords:
NEGF
GW
2D TMDs
DFT

ABSTRACT

Within the framework of many-body perturbation theory integrated with density functional theory (DFT), a novel defect-subspace projection GW method, the so-called p-GW, is proposed. By avoiding the periodic defect interference through open boundary self-energies, we show that the p-GW can efficiently and accurately describe quasi-particle correlated defect levels in two-dimensional (2D) monolayer MoS_2. By comparing two different defect states originating from sulfur vacancy and adatom to existing theoretical and experimental works, we show that our GW correction to the DFT defect levels is precisely modeled. Based on these findings, we expect that our method can provide genuine trap states for various 2D transition-metal dichalcogenide (TMD) monolayers, thus enabling the study of defect-induced effects on the device characteristics of these materials *via* realistic simulations.

1. Introduction

The physical dimension of Si logic transistors is approaching the atomic limit, thus requiring novel architectures and/or high-mobility channel materials for future technology nodes. Logic switches based on two-dimensional (2D) transition-metal dichalcogenide (TMD) monolayers have thus been proposed to continue Moore's scaling law, thanks to their remarkable electronic properties. However, several works [1,2] reported that various defects inside these monolayers may limit their performance as logic devices, mainly through charged impurity scattering and defect-induced trap levels. In particular, the "mid-gap" states introduced by those impurities are presumably at the origin of large Schottky barriers (SB) and high contact resistances. Therefore, in order to understand the physics related to defects in 2D TMD monolayers and to guide device design, *ab initio* simulations are required. In this work, we propose an efficient GW algorithm combined with density functional theory (DFT) to accurately describe defect levels in 2D TMD monolayers. In conventional GW calculations, environmental effects from substrates are included to obtain the realistic bandgap of 2-D monolayers, which requires huge computational resources [3]. Our method, so-called projected GW (p-GW), overcomes this issue by projections onto a defect subspace while removing spurious interactions between periodic images by means of open boundary conditions. This algorithm can correctly predict the position of defect levels in the bandgap and ensure efficiency by resorting to the DFT-level bandgap. We then apply this method to the most common defects in MoS_2 monolayers: S vacancy and adatom.

2. p-GW algorithm

The p-GW algorithm is based on Green's function theory and aims at describing isolated defects. We consider a device region Ω_D containing a defect and consisting of integer repetitions of a unit cell called "principal layer" (PL), as illustrated in Fig. 1. p-GW yields a device Green's function $\mathbf{G}_D$ which couples to the Bloch states of the host material at the boundaries and includes the correlation of the electrons localized around the defect. The algorithm is summarized in Fig. 2. The starting point is a DFT calculation of Ω_D with periodic boundary conditions (PBCs). From the DFT Hamiltonian and overlap matrices we replace the matrix elements connecting the boundaries with an energy-dependent boundary self-energy $\mathbf{\Sigma}_B$. Correlations are included via GW theory [4] only in a narrow region $\Omega_C \subset \Omega_D$ surrounding the defect where the GW self-energy $\mathbf{\Sigma}_{GW}$ is computed.

2.1. Boundary self-energy

The boundary self-energy $\mathbf{\Sigma}_B$ describes the coupling of Ω_D with the electrons in the Bloch states of the host material. It is efficiently computed from a k-point DFT calculation of the PL [5,6]. The algorithm

☆ The review of this paper was arranged by Francisco Gamiz.

* Corresponding author.
E-mail address: gandusgui@gmail.com (G. Gandus).

https://doi.org/10.1016/j.sse.2022.108499

Available online 5 November 2022

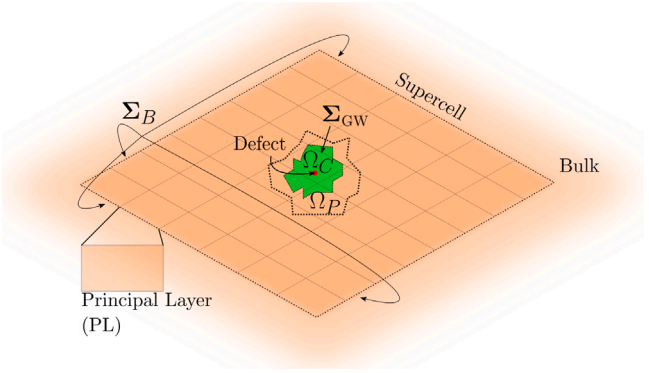

Fig. 1. Schematic view of a device region Ω_D containing a defect and consisting of integer repetitions of a PL. The boundary self-energy $\mathbf{\Sigma}_B$ describes the interaction of Ω_D with the hosting material and is used to describes the system with OBCs. GW corrections are calculated only in a narrow region Ω_C surrounding the defect and included in the p-GW algorithm via a GW self-energy $\mathbf{\Sigma}_{GW}$. The screened interaction used to calculate $\mathbf{\Sigma}_{GW}$, however, includes screening processes arising from the formation of electron–hole pairs in a larger polarization region Ω_P.

articulates itself around four sequential steps which are described in the following with the visual aid of Fig. 3. First, we perform a partial Bloch sum, along one direction, of the PL Hamiltonian and overlap matrices $\mathbf{H}_k, \mathbf{S}_k$ calculated on the k-grid for two consecutive cells, i.e. we obtain $\mathbf{H}_{0,k_t}, \mathbf{H}_{1,k_t}$ and similarly for the overlap, where k_t is a k-point in the remaining (transverse) direction. Those matrices are used to compute the surface Green's functions $\mathbf{\Sigma}_{k_t}^{L/R}$ [7], independently, for each k_t. Second, we construct the Green's function of a row of PLs with the same number repetitions that make up Ω_D in that direction. Here, OBCs are included via the calculated $\mathbf{\Sigma}_{k_t}$'s. Third, we expand the row of PLs in the transverse direction with a partial Bloch sum to obtain the Green's function $\mathbf{G}(z)$ of the pristine Ω_D region with OBCs. Finally, we calculate the boundary self-energy $\mathbf{\Sigma}_B(z)$ from the Dyson equation

$$\mathbf{\Sigma}_B(z) = z\mathbf{S} - \mathbf{H} - \mathbf{G}^{-1}(z), \tag{1}$$

where z is a complex energy with an infinitesimal shift along the imaginary axis and $\mathbf{H}$ and $\mathbf{S}$ are the Hamiltonian and overlap of the pristine Ω_D obtained from $\mathbf{H}_k, \mathbf{S}_k$ similar to $\mathbf{G}(z)$.

This efficient and precise algorithm allows us to treat the system as "open" and effectively simulates the defect as isolated. Indeed, this avoids undesired interferences or bound state patterns related to the PBCs.

2.2. GW self-energy

The GW self-energy $\mathbf{\Sigma}_{GW}$ is computed only for a narrow region Ω_C around the defect, as shown in Fig. 1. Ω_C includes the set of atoms with orbitals having a non-negligible contribution to the defect level states. The interaction among electrons in Ω_C on the other hand is calculated including screening processes arising from the formation of electron–hole pairs in a larger polarization region $\Omega_P \supset \Omega_C$. Due to the strong atomic character of the defect level states, Ω_P extends to the immediate vicinity of Ω_C. $\mathbf{\Sigma}_{GW}$ is obtained by a two-step projection of $\mathbf{G}_D$. The projection is defined such that the resulting subspace is orthogonal to the rest:

$$\mathbf{G}_X = \mathbf{S}_X^{-1}\mathbf{S}_{XD}\mathbf{G}_D\mathbf{S}_{DX}\mathbf{S}_X^{-1}. \tag{2}$$

Here, X is a subspace of D, $\mathbf{S}_X$ is the overlap matrix of X and $\mathbf{S}_{XD}$ between X and D. This choice is essential when extracting physical quantities associated with the subspace [5,8–10]. A first projection is performed onto Ω_P and yields $\mathbf{G}_P$. From $\mathbf{G}_P$ we compute the polarizability from which the screened Coulomb interaction $\mathbf{W}_P$ can be calculated in the random phase approximation (RPA) [11,12]. A second projection onto Ω_C gives $\mathbf{G}_C$ which is multiplied by the part of the screened interaction $\mathbf{W}_P$ in Ω_C, $\mathbf{W}_C$, to obtain $\mathbf{\Sigma}_{GW}$.

2.3. Self-consistency

The device Green's function $\mathbf{G}_D$ with OBCs and GW corrections can be written as

$$\mathbf{G}_D(z) = \left(z\widetilde{\mathbf{S}}_D - \widetilde{\mathbf{H}}_D - \mathbf{\Sigma}_B(z) - \mathbf{S}_{DC}\mathbf{S}_C\mathbf{\Sigma}_C(z)\mathbf{S}_C\mathbf{S}_{CD}\right)^{-1}, \tag{3}$$

where $\widetilde{\mathbf{H}}_D$ and $\widetilde{\mathbf{S}}_D$ are the device Hamiltonian and overlap matrices with removed PBCs and

$$\mathbf{\Sigma}_C(z) = -\mathbf{V}_{xc} + \mathbf{\Sigma}_{GW}(z) + \delta\mathbf{V}_H, \tag{4}$$

where $\mathbf{V}_{xc}$ is the DFT exchange–correlation (XC) potential that needs to be subtracted to avoid double counting of the correlations included in $\mathbf{\Sigma}_{GW}$. $\delta\mathbf{V}_H$ is the deviation from the DFT Hartree potential and is calculated from the change in the density matrix $\mathbf{D}_C$ in the Ω_C region. Because $\delta\mathbf{V}_H$ and $\mathbf{\Sigma}_{GW}$ depend on $\mathbf{G}_D$ themselves, Eq. (3) is solved self-consistently until convergence of $\mathbf{D}_C$.

3. Results

We study the effect of S vacancies (S-) and adatoms (S+) in 2D MoS_2 monolayers. The device region is composed of 4×6 repetitions of a PL composed of 6 Mo and 12 S atoms, as shown in Fig. 1. The electronic structure calculation of the PL is over-sampled with a $11 \times 6 \times 1$ k-mesh to obtain a $\mathbf{\Sigma}_B$ that precisely describes the bulk MoS_2 states. The polarization region Ω_P is shown in Figs. 4 and 5 together with the wavefunction of the states created by the defect. Ω_P includes up to the 2nd nearest neighbor to Ω_C, i.e. 12 Mo and 13 S atoms for S- and 3 Mo and 15 S atoms for S+. The defect states have a strong atomic orbital character: they are essentially a superposition of the $3d$ Mo orbitals closest to the vacancy for S- and an unpaired electron in the in-plane p orbital of the S adatom for S+. This allows us to define Ω_C as the 3 Mo and their surrounding S atoms for S- and the single S adatom for S+. $\mathbf{\Sigma}_C$ is then computed in this region only.

We calculated the corresponding density-of-states (DOS), the projected DOS (PDOS), and the electron transmission and report these results in Fig. 6. It is apparent from the DOS and the PDOS that the effect of the many-body correction is to shift the energy levels of the defect while preserving the DFT properties, i.e. the bandgap, as also corroborated by the conservation of the bulk-like electronic transmission. The DFT study for S- reveals that the dangling bonds left by the vacancy trigger the emergence of an unoccupied deep state at 0.4 eV below the conduction band minima (CBM), which is shifted down by an additional 0.2 eV from the GW correction. Recently an experimental investigation of defects in MoS_2 flakes [13] revealed deep level states around 0.8 eV below the CBM associated with S vacancies, which clearly indicates the correct trend of the GW correction. Previous k-point GW studies of full defect+MoS_2 S- structures found values of the defect level position with respect to the CBM [3] similar to our calculations. This indicates that our p-GW algorithm can accurately predict trap-levels with minimal computational burden. The DFT study for S+ predicts a shallow state close to the valence band. The GW correction pulls the defect-level position down into the valence band, as suggested by experimental studies that show a strong p-type behavior in the presence of S adatoms [14]. This indicates that such defects may act as doping center, a behavior that is not captured by pure DFT.

4. Conclusions

We proposed a novel algorithm to locally and efficiently apply many-body corrections using GW to a region surrounding a defect. Periodic self-interactions are removed by virtue of an efficient boundary self-energy calculation. The presented algorithm is then applied to S vacancy and adatom defects in a MoS_2 monolayer. Our method is a first step toward the inclusion of many-body methods beyond DFT in large scale simulations of realistic devices.

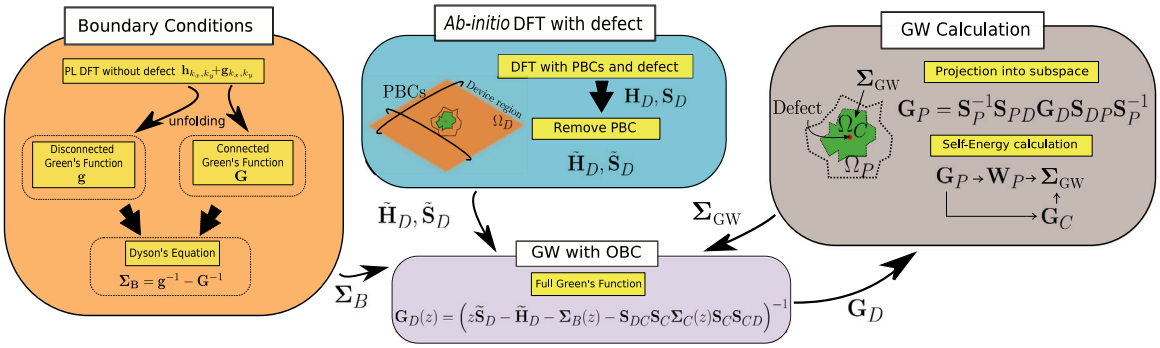

Fig. 2. Flowchart of the p-GW method for efficient modeling of defected structures with GW corrections. (Orange box) $\mathbf{\Sigma}_B$ is constructed from the DFT calculation of a periodic PL. (Blue box) The $\widetilde{\mathbf{H}}_D$ and $\widetilde{\mathbf{S}}_D$ of the defected region are obtained from a separate DFT calculation by removing the PBCs. (Gray box) $\mathbf{\Sigma}_{GW}$ is computed for a subspace containing the defect where $\mathbf{G}_C$ is constrained to the defect and $\mathbf{W}_P$ includes its surroundings. (Purple box) Equation for the full Green's function coupling all boxes. (For interpretation of the references to color in this figure legend, the reader is referred to the web version of this article.)

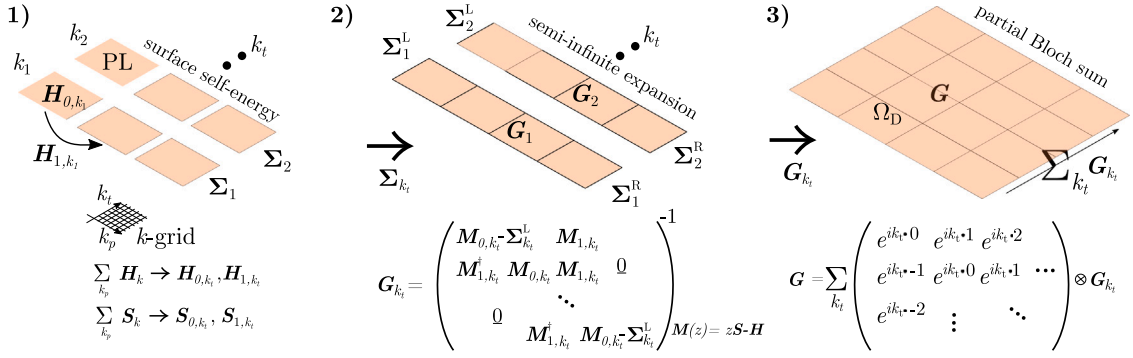

Fig. 3. Steps summarizing the construction of the connected Green's function $\mathbf{G}$ starting from the Hamiltonian and overlap matrices, $\mathbf{H}_k$ and $\mathbf{S}_k$, of a DFT calculation of a PL on a k-grid. (1) A partial Bloch sum of $\mathbf{H}_k$ and $\mathbf{S}_k$ is performed for two consecutive cells and the matrices $\mathbf{H}_{0,k_t}, \mathbf{H}_{1,k_t}, \mathbf{S}_{0,k_t}, \mathbf{S}_{1,k_t}$ are obtained. These serve to compute the surface Green's functions $\mathbf{\Sigma}_{k_t}^{L/R}$ at each k_t. (2) The Green's functions $\mathbf{G}_{k_t}$ of a row of PLs with OBCs is constructed for each k_t. (3) A partial Bloch's sum of $\mathbf{G}_{k_t}$ in the remaining direction leads to $\mathbf{G}$.

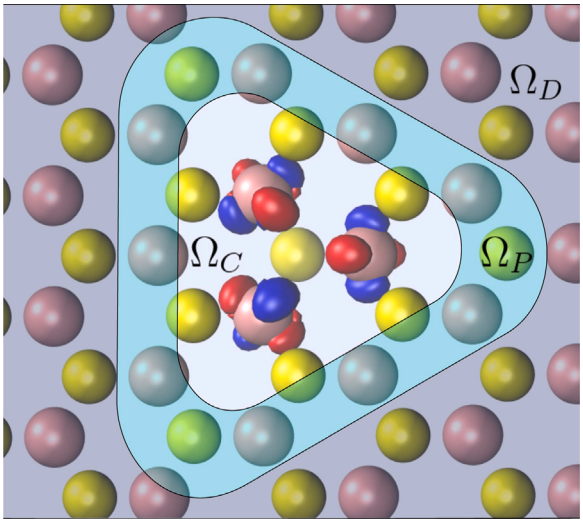

Fig. 4. Atomic structure of single S vacancy in MoS_2 monolayer. Gray spheres, Mo atoms; yellow, S atoms. The blue and red isosurfaces represent the wavefunction of the state created by the defect. The defect region Ω_C (white) is defined by the 3 Mo and their surrounding S atoms. The polarization region Ω_P (light blue) includes atoms up to the second nearest neighbor to Ω_C. (For interpretation of the references to color in this figure legend, the reader is referred to the web version of this article.)

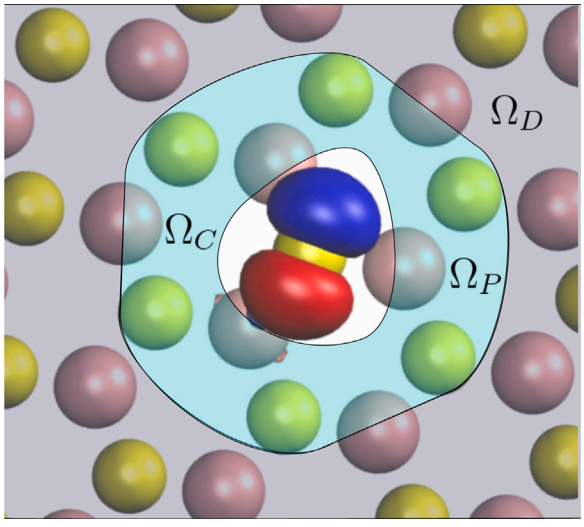

Fig. 5. Atomic structure of S adatom absorbed on top of MoS_2 monolayer. Gray spheres, Mo atoms; yellow, S atoms. The blue and red isosurfaces represent the wavefunction of the state created by the defect. The defect region Ω_C (white) is defined by the S adatom. The polarization region Ω_P (light blue) includes atoms up to the second nearest neighbor to Ω_C. (For interpretation of the references to color in this figure legend, the reader is referred to the web version of this article.)

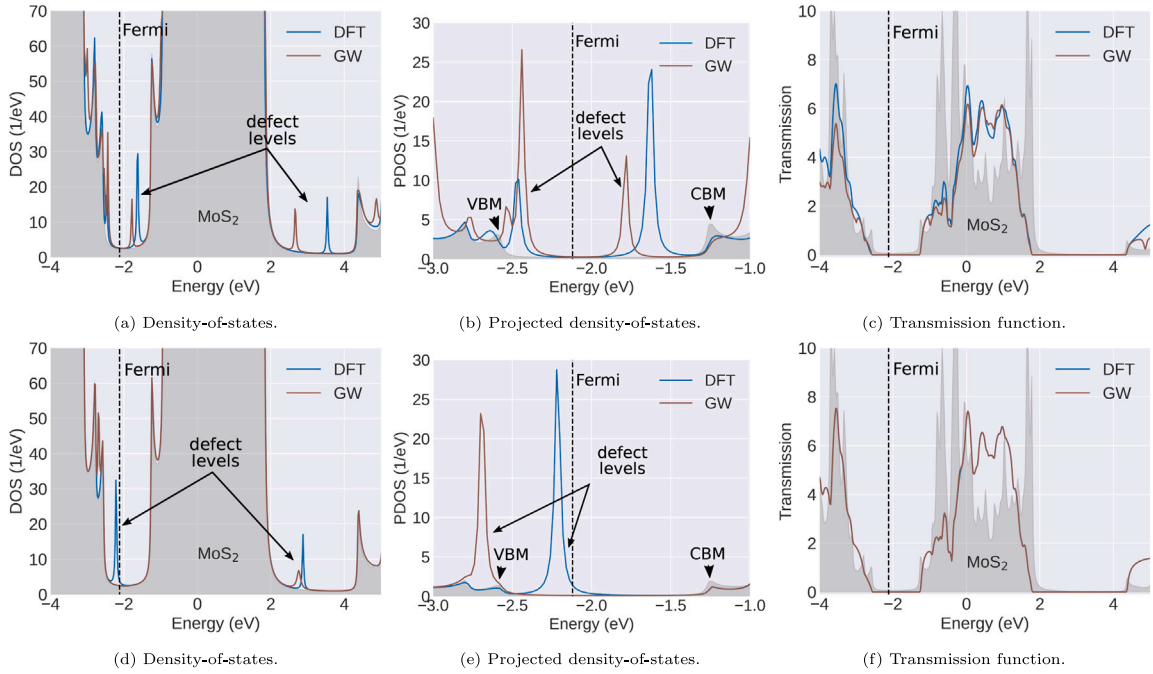

(a) Density-of-states. (b) Projected density-of-states. (c) Transmission function.

(d) Density-of-states. (e) Projected density-of-states. (f) Transmission function.

Fig. 6. Results for S- (a–c) and S+ (d–f) obtained by DFT and the proposed p-GW method. The shaded gray area represents the DOS of bulk MoS_2. The total density-of-states of the device region (a, d) and projected onto the GW subspace (b, e) show that the many-body correction shifts the defect level states while maintaining the DFT bulk properties. (c, f) Transmission function through the defected structure. The onset of the electron transmission around the fundamental gap is also preserved by the p-GW correction. (For interpretation of the references to color in this figure legend, the reader is referred to the web version of this article.)

Declaration of competing interest

The authors declare that they have no known competing financial interests or personal relationships that could have appeared to influence the work reported in this paper.

Data availability

Data will be made available on request.

Acknowledgments

This work was supported by the NCCR MARVEL funded by the Swiss National Science Foundation grant 51NF40-205602. Computational support from the Swiss Supercomputing Center (CSCS) under project ID s1119 is gratefully acknowledged.

References

[1] Rai A, Roy A, Valsaraj A, Chowdhury S, Taneja D, Wang Y, et al. Chapter 11 - Devices and defects in two-dimensional materials: Outlook and perspectives. In: Addou R, Colombo L, editors. Defects in two-dimensional materials. Materials today, Elsevier; 2022, p. 339–401. http://dx.doi.org/10.1016/B978-0-12-820292-0.00017-3.

[2] Lee Y, Fiore S, Luisier M. Ab initio mobility of single-layer MoS 2 and WS 2: Comparison to experiments and impact on the device characteristics. In: 2019 IEEE international electron devices meeting. IEDM, IEEE; 2019, p. 24–4.

[3] Naik MH, Jain M. Substrate screening effects on the quasiparticle band gap and defect charge transition levels in MoS 2. Phys Rev Mater 2018;2(8):084002.

[4] Hedin L. New method for calculating the one-particle Green's function with application to the electron-gas problem. Phys Rev 1965;139(3A):A796.

[5] Gandus G, Lee Y, Passerone D, Luisier M. Efficient partitioning of surface Green's function: Toward ab initio contact resistance study. In: 2020 International conference on simulation of semiconductor processes and devices. SISPAD, IEEE; 2020, p. 177–80.

[6] Papior N, Calogero G, Leitherer S, Brandbyge M. Removing all periodic boundary conditions: Efficient nonequilibrium Green's function calculations. Phys Rev B 2019;100(19):195417.

[7] Sancho ML, Sancho JL, Sancho JL, Rubio J. Highly convergent schemes for the calculation of bulk and surface Green functions. J Phys F: Metal Phys 1985;15(4):851.

[8] Jacob D. Towards a full ab initio theory of strong electronic correlations in nanoscale devices. J Phys: Condens Matter 2015;27(24):245606.

[9] Soriano M, Palacios J. Theory of projections with nonorthogonal basis sets: Partitioning techniques and effective Hamiltonians. Phys Rev B 2014;90(7):075128.

[10] O'Regan DD. Subspace representations in ab initio methods for strongly correlated systems. In: Optimised projections for the Ab initio simulation of large and strongly correlated systems. Springer; 2012, p. 89–123.

[11] Strange M, Rostgaard C, Häkkinen H, Thygesen KS. Self-consistent GW calculations of electronic transport in thiol- and amine-linked molecular junctions. Phys Rev B 2011;83:115108. http://dx.doi.org/10.1103/PhysRevB.83.115108, URL https://link.aps.org/doi/10.1103/PhysRevB.83.115108.

[12] Rostgaard C, Jacobsen KW, Thygesen KS. Fully self-consistent GW calculations for molecules. Phys Rev B 2010;81(8):085103.

[13] Srivastava S, Mohapatra YN. Defect density of states in natural and synthetic MoS2 multilayer flakes. J Phys D: Appl Phys 2022;55(34):345101.

[14] Addou R, Colombo L, Wallace RM. Surface defects on natural MoS2. ACS Appl Mater Interfaces 2015;7(22):11921–9.